Lab on a Chip

Cite this: *Lab Chip*, 2011, **11**, 3458

www.rsc.org/loc

PAPER

A microfluidic device that generates hydroxyl radicals to probe the solvent accessible surface of nucleic acids

Christopher D. Jones,†[a] Jörg C. Schlatterer,†[b] Michael Brenowitz*[b] and Lois Pollack*[a]

Received 1st April 2011, Accepted 28th July 2011
DOI: 10.1039/c1lc20280d

We describe a microfluidic device containing a mineral matrix capable of rapidly generating hydroxyl radicals that enables high-resolution structural studies of nucleic acids. Hydroxyl radicals cleave the solvent accessible backbone of DNA and RNA; the cleavage products can be detected with as fine as single nucleotide resolution. Protection from hydroxyl radical cleavage (footprinting) can identify sites of protein binding or the presence of tertiary structure. Here we report preparation of micron sized particles of iron sulfide (pyrite) and fabrication of a microfluidic prototype that together generate enough hydroxyl radicals within 20 ms to cleave DNA sufficiently for a footprinting analysis to be conducted. This prototype enables the development of high-throughput and/or rapid reaction devices with which to probe nucleic acid folding dynamics and ligand binding.

Introduction

Protection analysis (footprinting) with hydroxyl radicals (·OH) has long been a valuable tool for the study of DNA and RNA structure and complexes of nucleic acids with proteins (Fig. 1).[1–4] When used as a footprinting probe, ·OH reports the solvent accessible surface in solution of the phosphodiester backbone of nucleic acid with as fine as single nucleotide resolution. Fenton based ·OH footprinting has been applied to time-resolved analysis of RNA folding[5] and the structural analysis of proteins.[6–8] The inspiration for our novel approach to ·OH footprinting is studies of the origin of life[9] and environmental toxicology[10,11] demonstrating the ability of the iron sulfide mineral pyrite to catalyze the production of ·OH in solution from dissolved oxygen and cleave nucleic acid.

Our approach exploits the advantages of microfluidic systems: small sample volumes, short reaction times and the potential for multiplexed and/or high throughput applications. Iron sulfide (pyrite) micro-particles are captured by a constriction in a micro-channel. Hydrogen peroxide (H_2O_2) flowing through the pyrite matrix generates sufficient quantities of to cleave co-flowing nucleic acid with the single-hit kinetics necessary for footprinting. Because the lifetime of ·OH is quite short (half life $\sim 10^{-9}$ s),[12] the amount of sample cleavage by ·OH is determined by the rate of its passage through the pyrite matrix. We demonstrate the efficacy of this device for footprinting on the millisecond time scale, and discuss how it can be incorporated into mixers and/or parallelized for high-throughput sample analysis.

Experimental

Pyrite particle preparation

Pyrite was purchased from Ward's Natural Sciences (Rochester, NY). Nuggets of the mineral were crushed into 0.3 to 0.8 cm pieces by mortar and pestle, ground by a Retsch PM100 ball grinder and sieved using a Retsch AS200 sieving station.[9] Fine particulates were removed by filtration through a 40 μm sieve drawn by vacuum (Millipore Steriflip SCNY0040). Approximately 8 g of ground pyrite with a particle size distribution of 40–63 μm are obtained from 100 g of raw mineral.

Device design and fabrication

The microfluidic device consists of a single linear channel (200 μm × 100 μm × 1 cm), with a constriction in the middle to trap the pyrite particles (Fig. 2). The device is fabricated from Zeonor (1020R, Zeon Chemicals L.P., Louisville, KY) at the Cornell NanoScale Science and Technology Facility (CNF, Ithaca, NY). Positive Si wafer masters of our device channel geometry are made using standard photolithography and plasma etching techniques.[14] A Si wafer containing four masters is placed on a hot press with a ~2 cm square piece of 2 mm thick Zeonor on top of each master. We press at 135 °C and 750 psi for 10 min. Inlet and outlet holes at the ends of the channels are punched with a custom die set.

The Zeonor devices are sealed by applying a piece of clear one sided polyester pressure sensitive tape (ARseal 90697, Adhesives Research, Glen Rock, PA).[15] The resulting device has excellent optical clarity and high resistance to chemical decomposition (except

[a]*School of Applied and Engineering Physics, Cornell University, Ithaca, NY, USA. E-mail: lp26@cornell.edu; Fax: +1 607 255 7658; Tel: +1 607 255 8695*
[b]*Department of Biochemistry, Albert Einstein College of Medicine, Bronx, NY, USA. E-mail: michael.brenowitz@einstein.yu.edu; Fax: +1 718 430 8565; Tel: +1 718 430 3179*
† Authors made equal contribution.

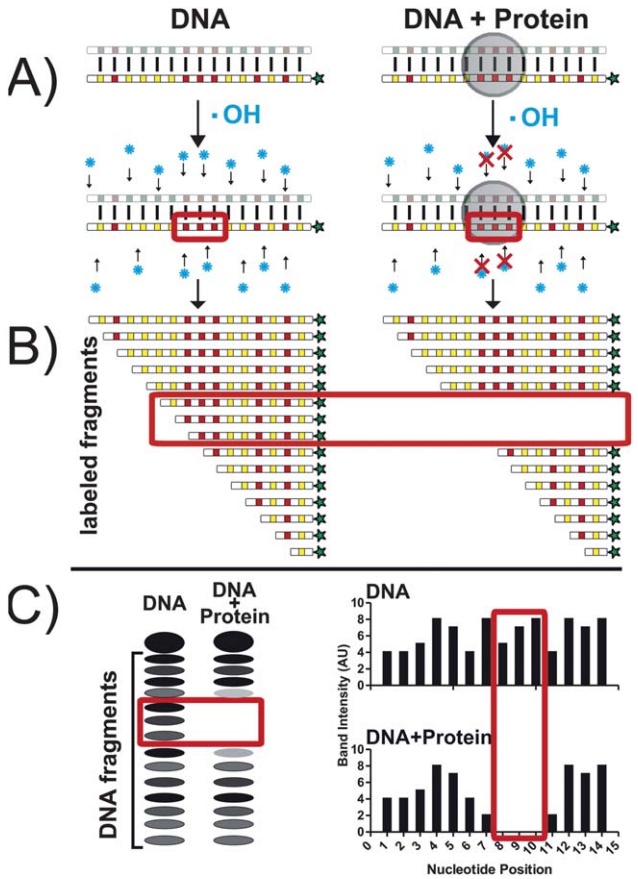

Fig. 1 Hydroxyl radical footprinting of DNA structure and a DNA-protein interaction. (A) Hydroxyl radicals (blue) attack DNA (left) and a DNA-protein complex (right). The strand specific label is shown as star. The detection method exclusively monitors the labeled DNA fragments. The gray disk indicates a protein which binds to the DNA. (B) Robust protection of the DNA from ·OH cleavage is observed at the nucleotides involved in protein complex formation since the concentration of fragments terminating in protected nucleotides is diminished. (C) Gel electrophoretic separation of footprinted DNA and subsequent imaging shows fragments as dark bands with potentially different degrees of shading. The concentration of cleavage fragments is proportional to solvent exposure. Subtle variation in the ·OH cleavage pattern of the free DNA duplex reflects sequence dependent differences in structure.[13]

that the tape adhesive is soluble in acetone). This method yields devices without leaks or clogs that remain sealed over a wide range of flow rates. The use of tape enables more efficient positioning of the pyrite particles, if the particles get stuck in the adhesive at an undesirable location or clog, that region can be surgically removed and "patched" with another piece of tape. Using this technique, embossed devices can be sealed with nearly 100% efficiency about one hundred times faster than with curable silicones.

To load the sealed device, it is placed in a holder that interfaces with an external fluid handling system.[16] About 5 mg of pyrite particles are suspended in ~10 mL of nanopure deionized water. This solution flows by gravity into the inlet until a 1–3 mm long plug of pyrite forms at the constriction. The holder is also used to position the device on a translation stage for characterization by confocal microscopy.

To create the free-standing device used for DNA cleavage experiments, tubing is inserted into the inlet and outlet channels and glued into place with TorrSeal epoxy. The entire device is then potted in poly(dimethylsiloxane) (PDMS). The PDMS seals the device but does not interfere with its optical transparency. Pyrite surface oxidation is reduced by flowing 0.5 M HCl through the device at rates of 5–100 μL min^{-1} for 1 h.[9] This acid rinse is followed by a ~30 min flow of degassed nanopure deionized water for dye studies, or degassed DEPC treated water (Ambion) for DNA studies.

Sample preparation

Dye. A 60 mL syringe is filled with 1.25 μM fluorescein and 1% H_2O_2 dissolved in degassed nanopure DI water. The syringe is wrapped in aluminum foil to shield the dye from light. Degradation of fluorescein by ·OH results in a loss of emission intensity and is used to assess radical production within the device.[5]

DNA. The 54 base DNA sequence AATAGATAGGTA GACCTTTACAAGTTTTCCCTGGGCCTATAGTGAGTCG TATTA and its complement was obtained from IDT. The DNA strands are annealed and purified by standard procedures.[17,18] The top strand (sequence provided above) is end labeled with ^{32}P so that a unique set of cleavage products can be visualized;[19] 10 pmol of DNA are 5′-labeled with ^{32}P by standard kinasing reaction (buffers and enzymes from New England Biolabs),[20] gel purified and precipitated by ethanol and dried. The ^{32}P-DNA is re-suspended in degassed water and added to its unlabeled complement to a final duplex concentration of 100 μM. The duplex is annealed by incubation at 90 °C for 2 min followed by cooling on ice for 10 min. The solution contains a ~1.15 molar excess of unlabeled complement. The ^{32}P-DNA is stored at 4 °C for up to 2 weeks. For experiments, aliquots of the stock solution were dissolved to 0.6 μM in sodium cacodylate buffers (pH 7.4) and degassed. H_2O_2 diluted into the same buffer was added to the indicated concentration just prior to initiating an experiment.

Experimental set-up

Dye degradation. To assay ·OH production by fluorescein degradation[5] a device in a sample holder is mounted on an Olympus FV1000 confocal microscope (Fig. 3a) using an excitation wavelength of 488 nm. A syringe pump (Harvard Apparatus PHD 2000) pushes dye through the device. After the device is centered in the beam, the flow rate is stabilized at 50 μL min^{-1} and a set of images acquired (Fig. 3b). Regions of interest (ROI) are defined on either side of the pyrite. These areas are equidistant from the edges of the frame, inside the boundaries of the channel profile, as large as possible and the same size. Hydroxyl radical production is calculated by dividing the mean intensity of the post- and pre-pyrite ROIs, yielding the fraction of dye fluorescence lost.

DNA fragmentation. A Harvard Apparatus 11 Plus syringe pump drives solution containing ^{32}P-DNA through a standalone device (Fig. 2). A 30 μL sample, injected into a short length of inlet tubing, is surrounded on both sides by small air bubbles to isolate the sample. Once the sample is in place, the inlet tubing is connected to a 1 mL syringe filled with degassed DEPC treated water, and flow is initiated. The sample is pushed through the device, where ·OH cleavage occurs, and into a short length of

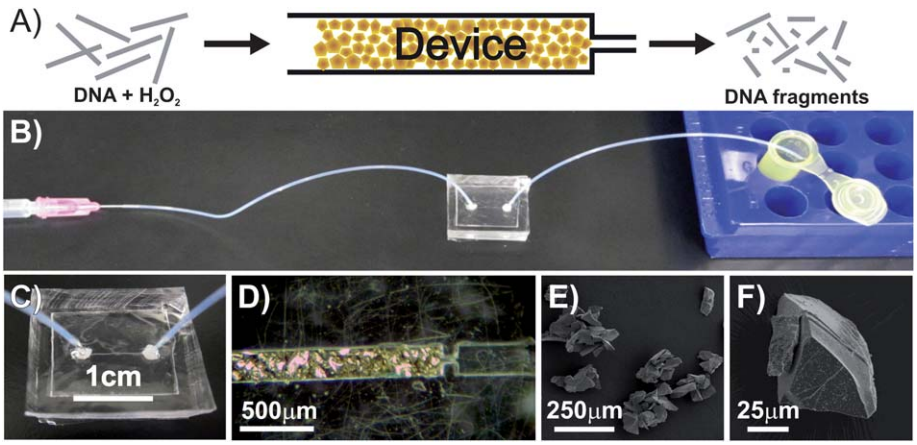

Fig. 2 Device setup and pyrite particle characterization. (A) Full-length DNA duplex and H_2O_2 are pushed into the device. After passing through the pyrite matrix, single strand nicks are introduced into the duplex DNA. These strands are separated prior to electrophoretic separation. This figure shows the fragments of varying length obtained after denaturation of the DNA duplex. (B) A syringe pump drives the DNA/H_2O_2 solution through the PDMS potted device, and into a microfuge tube. (C) Photograph of a device potted in PDMS, showing the TorrSeal epoxy for inlet and outlet tubing. (D) Photomicrograph of pyrite in device; channel width is 200 μm. (E) Aggregates of pyrite particles in SEM micrograph, and (F) A single pyrite particle.

outlet tubing. The end of the tubing is immersed in 300 μL of absolute ethanol in a microfuge tube to eliminate droplet formation at the outlet which would disrupt the flow (Fig. 2).

Complete passage of the sample through the device and into the tube is ensured by monitoring the position of the air bubbles and double checked with a Geiger counter. The microfuge tube is capped and immersed in dry ice to precipitate the ^{32}P-DNA.[21] The ^{32}P-DNA cleavage products are separated from the full-length molecule by electrophoresis on a 15 cm long 15% denaturing polyacrylamide gel.[22] Gels are imaged using a phosphor storage plate and scanner (Molecular Dynamics, Storm 820). The fraction of DNA fragments is calculated from the ratio of the box volumes (Molecular Dynamics, ImageQuant v5.2) enclosing all cleaved fragments, to the total intensity of fragmented and full length sample.[23] The 15 cm gels such as shown in Fig. 4 are useful only to separate the full-length DNA from the ·OH fragments. However, the ease with which the small gels can be cast and dried and their short run time makes them a boon to dose-response determinations for optimization of experiments.

Single nucleotide resolution of the ·OH fragmentation products is achieved using a standard 45 cm sequencing gel. Quantification of the intensity of each fragment band is conducted using the Semi-Automated Footprinting Analysis (SAFA) software.[24] Protection profiles were generated by internal normalization of the band volumes included in the boxes of a sample lane (Fig. 5b). The line profiles shown in Fig. 5c were generated using a line width of eleven (ImageQuant v5.2). Footprinting of DNA was performed according to standard procedures[25] that include mixing Fe-EDTA, sodium L-ascorbate, and H_2O_2 to produce hydroxyl radicals.[26,27] The mean and standard deviation of three lanes are shown in Fig. 5b.

Fluid flow characterization

The flow rate of 50 μL min^{-1} selected for these studies yields an estimated Reynold's number well below one in both the open channel and the pyrite-containing region indicating laminar flow.[28] To estimate the interaction time with the packed pyrite, we assume that the particles fill the channel like random close packed spheres, yielding a packing fraction of 64%. Although calculation of random packing fractions of objects with non-spherical shape is fundamentally difficult,[29] the range of available fractions is still rather limited, with the absolute maximum (and unlikely) packing fraction only 15% higher.[30] The linear flow speed in the pyrite-free portion of the device (the left-most part of the channel shown in Fig. 2A, center panel) is calculated to be 4.2 cm/s. Using the hard sphere random close packing assumption to model the decrease in channel volume due to the presence of pyrite, we compute a flow speed of 11.5 cm s^{-1} in the pyrite-containing region. Thus, an estimate of the interaction time of the flowing solution with the pyrite can be obtained by dividing the length of the channel that contains pyrite particles (along the flow direction) by the flow speed. Using the value for flow speed given above, this interaction time is less than 10 ms per mm of packed pyrite.

Results

We demonstrate that a microfluidic device containing particles of pyrite can produce ·OH at concentrations sufficient for structural studies of nucleic acids and rapidly enough for time-resolved analysis. Pyrite surfaces generate substantial quantities of ·OH in aqueous solution that can cleave nucleic acids. While the mechanism by which pyrite generates ·OH is not fully understood, the most plausible reaction sequence is

$$\mathrm{Fe(II)} + \mathrm{O_2} \rightarrow \mathrm{Fe(III)} + \cdot(\mathrm{O_2})^- \quad (1)$$

$$\mathrm{Fe(II)} + \cdot(\mathrm{O_2})^- + 2\mathrm{H^+} \rightarrow \mathrm{Fe(III)} + \mathrm{H_2O_2} \quad (2)$$

$$\mathrm{Fe(II)} + \mathrm{H_2O_2} \rightarrow \cdot\mathrm{OH} + \mathrm{OH^-} + \mathrm{Fe(III)}. \quad (3)$$

The hypothesis that we tested in this study is that controlled exposure of nucleic acid to pyrite particles yields the cleavage necessary for footprinting. We find that the necessary and sufficient ·OH concentration is achieved in the desired time scale

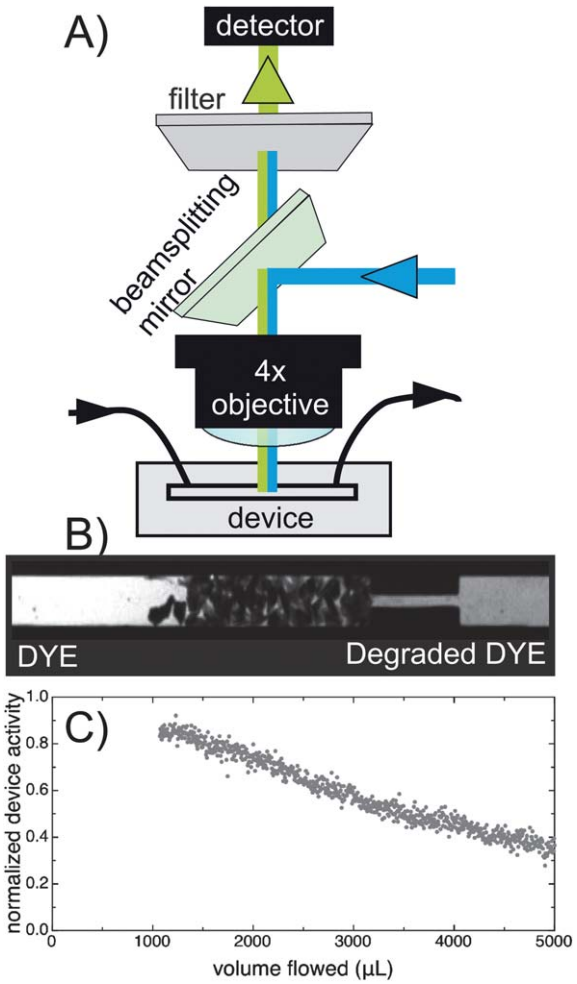

Fig. 3 Confocal microscopy set-up and results. (A) Schematic of microscope where the absorption laser light bounces off a beam splitting mirror to go through the objective and illuminate the sample. The emitted light and some of the reflected excitation light return through the objective and beam splitter. A filter excludes the excitation wave-length before the emitted light hits a detector. (B) An example of our experimental data, with dye flowing from left to right. Prior to interaction with the pyrite (left side), the dye emission is brighter than in the post-pyrite region (right side). The shape and packing of the pyrite is observable in the center of the image. (C) Hydroxyl radical production by the pyrite matrix decays to one-half when 3500 μL of sample with H_2O_2 has flowed.

by adding H_2O_2 effectively skipping the first two steps of the reaction sequence summarized above.

Fluorescence detection of ·OH production

Because the analysis of ^{32}P-DNA degradation requires multiple post-exposure processing steps, optically assaying ·OH production within the device is an efficient way to develop and test device effectiveness and capability. The optical clarity of the device may prove beneficial to the development of devices that meld optical pumping and/or probing with footprinting and thus open new avenues of investigation. Loss of dye fluorescence was used to monitor ·OH production in the device as a function of mineral amount, solution flow rate, pH and buffer composition (data not shown). We found that pH had negligible impact on radical production between 5.0 and 7.5. The salient result from this survey of operational parameters is that substantial dye degradation is only observed when H_2O_2 is present when the solution flow is fast enough to ensure millisecond contact of the sample with the mineral matrix.

That a single device can effectively generate ·OH repetitively is shown in Fig. 3c. We continuously flowed dye and H_2O_2 containing solution through the device and recorded the decrease in fluorescence as a function of the solution volume. Dye degradation decreases linearly to ~50% when ~5 mL of solution has passed through the device. Since the volume of each DNA sample analysed is ~30 μL, tens of samples can be analysed before the functionality of the device becomes unacceptably low. The pyrite matrix can regain full functionality by HCl flushing and washing. These data suggest that repetitive use of a device will be limited by clogging due to matrix settling or externally introduced debris, macromolecule absorption or precipitation rather than loss of pyrite mediated catalysis.

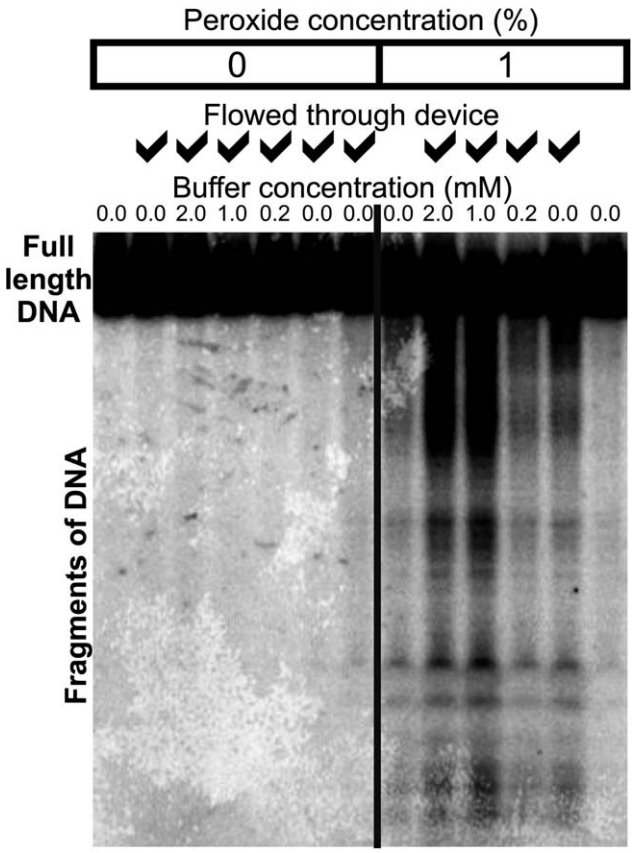

Fig. 4 Electrophoretic separation of full-length ^{32}P-DNA from the ·OH cleavage fragments by a short low resolution gel whose purpose is solely to separate the intact DNA from the ·OH cleavage reaction products. The left portion of the gel has no H_2O_2 present. No quantifiable fragments above background (denoted as lanes where the sample did not flow through the device) are detectable. In contrast, significant fragmentation is observed in the presence of H_2O_2 (right panel).

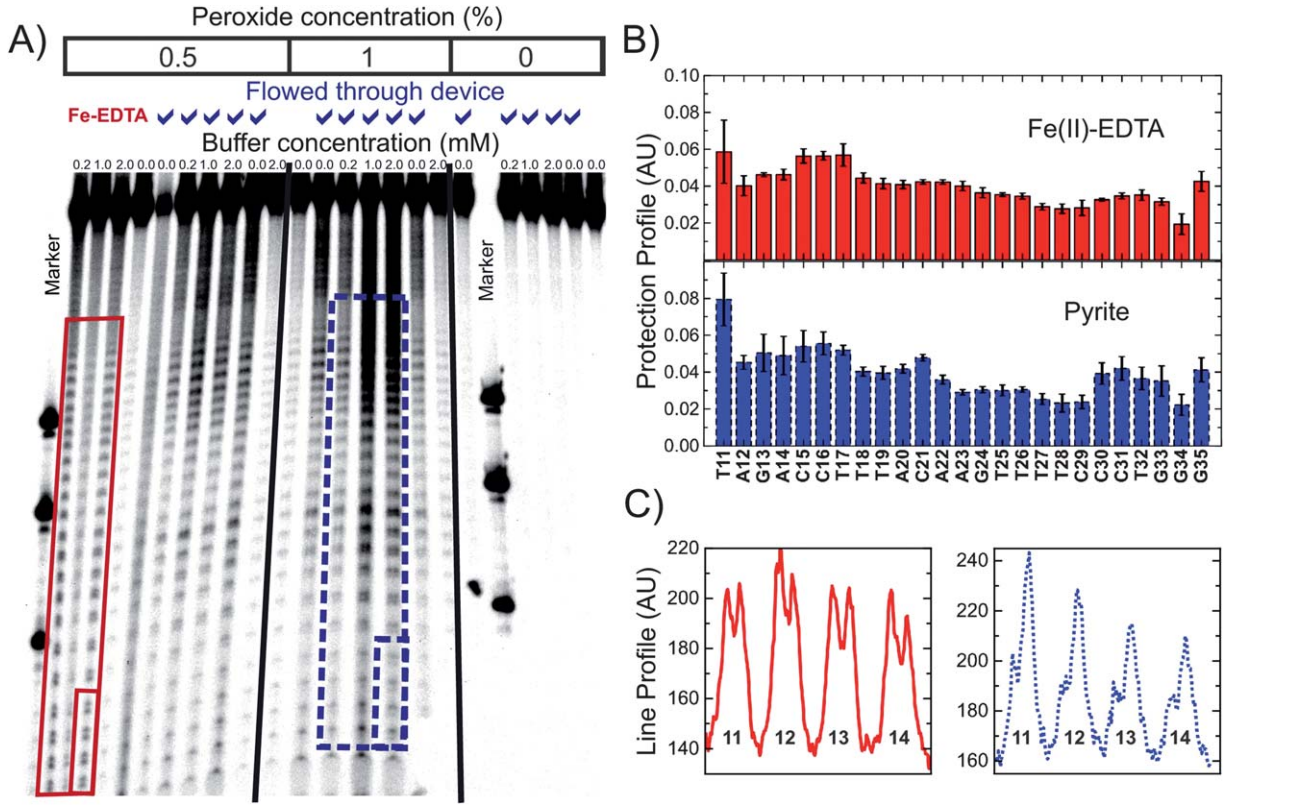

Fig. 5 Analysis of DNA fragments. (A) Separation of DNA fragments using a high resolution 45 cm sequencing gel. (B) Plot of averaged individual nucleotide band intensities for regions in (A) surrounded with boxes. The normalized band volumes are presented as protection profiles, where a low intensity would relate to a protection region, as in the case of protein binding (see Fig. 1C). DNA was fragmented by traditional Fe(II)-EDTA approach (top) and the new pyrite chip technology (bottom). The bands analyzed are marked in the top panel. The mean and standard deviation of three lines are shown. (C) Line profiles of nucleotides 11 through 14.

DNA fragmentation

Emboldened by the dye degradation assay demonstration of ·OH production when H_2O_2 is present in the sample within tens of ms, we analysed cleavage of a 54 bp ^{32}P-DNA duplex to determine whether nucleic acid footprinting is indeed feasible using our device. We first determined that the DNA was not significantly absorbed to mineral surface under our experimental conditions (^{32}P-DNA recovery = 84% ± 15; data not shown) since such absorption has been documented.[31]

The effluent from the device contains both full-length DNA and its fragmentation products. Electrophoretic separation of these ^{32}P-DNA populations followed by their quantification yields the ·OH fractional cleavage by which footprinting efficacy can be judged (Fig. 4). ^{32}P-DNA samples flowed through our device in the absence of H_2O_2 display no detectable fragmentation above the control. The addition of 1% H_2O_2 to the sample results in robust DNA fragmentation (Fig. 4). These results are completely consistent with the dye degradation analysis.

Twelve percent fragmentation is measured for the ^{32}P-DNA duplex in 1 mM pH 7.4 buffer and a flow rate of 50 μL min^{-1}; DNA cleavage increases with increasing H_2O_2 concentration through our probed range of up to 1% H_2O_2, (Fig. 6). A weak dependence on buffer concentration is observed. The 12% DNA fragmentation achieved with 1% H_2O_2 is appropriate for the conduct of footprinting studies. This amount of fragmentation yields good signal to background for clear fragment detection (Fig. 5b), uniform fragment distribution and is within the realm of single-hit kinetics which is required for accurate quantitation.[23,25,32] Not surprisingly, DNA fragmentation is affected by solution flow rate and the amount of pyrite in the device. As expected, the amount of fragmentation increases as more pyrite is added or as the flow rates decreases (Fig. 6b).

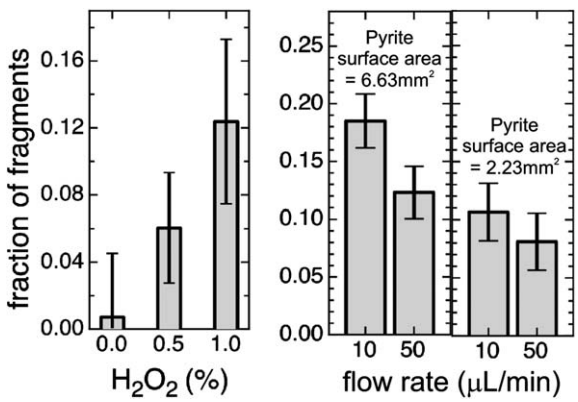

Fig. 6 DNA fragmentation results. Left plot: DNA fragmentation increases with increasing H_2O_2 concentration. Right plots: We observe a strong dependence on dose, resulting from either an increase in the accessible pyrite surface area, or an increase of interaction time resulting from slower flow rates.

Single-nucleotide separation of the ·OH cleavage fragments yields a profile of the solvent accessible surface of the phosphodiester backbone. Comparable profiles are observed between Fe(II)-EDTA and pyrite footprinting (Fig. 5b). Although the evidence is indirect, the comparability of the two profiles argues that indeed it is ·OH mediating both footprinting reactions. An interesting difference between Fe(II)-EDTA and pyrite footprinting is seen at the bottom of the gel where alternative cleavage products are resolved (Fig. 5a, small red and blue boxes). The line profile analysis of small fragments shows differences in the ratio of the alternative DNA cleavage products distinguishable with 5′ labelled DNA.[33] For Fe(II)-EDTA the 3′-phosphate and 3′-phophoglycolate products are roughly equivalent; in contrast, the 3′-phophoglycolate product apparently is in excess for pyrite footprinting (Fig. 5c). These results suggest bias in the preferred carbon that is attacked by the radical. Further exploration of the details of the reaction chemistry is beyond the scope of this article.

Taken together these results show that our pyrite packed device can degrade DNA on the millisecond time scale and that H_2O_2 concentration, solution flow rate and pyrite surface area can be tuned to provide the fragmentation necessary and sufficient for high-throughput and time resolved structural studies of nucleic acids.

Discussion and conclusions

We demonstrate the use of pyrite micro-particles confined in a microfluidic channel to generate ·OH that react with flowing DNA to map the solvent accessible surface of its phosphodiester backbone. The proof-of-principle device described here lays the groundwork for development of sophisticated microfluidic platforms for footprinting experiments. This powerful nucleic acid analytical technique has applications to biological questions including identifying and studying the binding of proteins to DNA and RNA and monitoring folding and structural transitions of DNA and RNA. Similar analyses can be carried on proteins. Although the device described here relies on silicon processing, sophisticated fabrication tools are not required to replicate this simple geometry. The design is fully compatible with convenient soft lithographic techniques allowing easy and inexpensive manufacturing.

We envision applications in numerous areas. The simplicity of device design ensures that it can be combined with other elements in either series or parallel arrangements. For example, this "reactor" can be placed downstream of rapid, microfluidic mixers, enabling time-resolved studies of reactions such as RNA or protein folding. Interaction time with ·OH should be minimized to achieve the sharpest possible time resolution. This time scale is easily controlled, either by constructing channels containing varying amounts of pyrite, or more simply, by varying the flow rate through a single channel. Based on the performance of our prototype, we anticipate achieving single digit millisecond time resolution for the footprinting reaction. In contrast to other time-resolved footprinting methods, the reaction self-terminates once the fluid has passed through the pyrite matrix; there is no need for quenching. The time resolution is sharp, clearly defined, and readily calibrated using fluorescence assays.

Another important application involves the development of high-throughput devices. If numerous channels are fabricated in parallel arrays, multiple experiments can be performed simultaneously. Because of the versatility of the microfluidic platform, these replicates can be identical, or can reveal differences in protections resulting from varying interaction times with radicals yielding a general measure of the extent of protection, or mixing with different chemical and/or macromolecular components. This proof-of-principle study employed the time consuming but direct method of gel electrophoresis to detect DNA fragments. Higher throughput detection can be achieved by utilization of capillary electrophoresis and its associated auto-sampling technology.[34–36] Finally, our device could be integrated with lab-on-a-chip modules that conduct the post-exposure processing necessary to visualize ·OH reaction products. Our versatile and simple-to-implement approach is readily combined with other fluidic elements, bringing a powerful new analytical tool to the chip.

Acknowledgements

The authors wish to thank Ina Pavlova for assistance with the confocal microscope, David Rigie for assistance with fabrication, and Suzette A. Pabit for assistance with embossing protocols. We also thank Einstein Summer Undergraduate Research Program (SURP) students Michael Shusterman and Yair Saperstein for their studies of ·OH cleavage of nucleic acids. This work was supported by the NSF through the IDBR program (Grant 0852796 to MB and 0852813 to LP) and the Cornell NanoScale Facility, a member of the National Nanotechnology Infrastructure Network (Grant ECS-0335765).

References

1 T. D. Tullius and B. A. Dombroski, *Science*, 1985, **230**, 679.
2 T. D. Tullius and B. A. Dombroski, *Proc. Natl. Acad. Sci. U. S. A.*, 1986, **83**, 5469.
3 J. A. Latham and T. R. Cech, *Science*, 1989, **245**, 276.
4 D. W. Celander and T. R. Cech, *Biochemistry*, 1990, **29**, 1355.
5 I. Shcherbakova, S. Mitra, R. H. Beer and M. Brenowitz, *Nucleic Acids Res.*, 2006, **34**, e48.
6 E. Heyduk and T. Heyduk, *Biochemistry*, 1994, **33**, 9643.
7 M. Zhong, L. Lin and N. R. Kallenbach, *Proc. Natl. Acad. Sci. U. S. A.*, 1995, **92**, 2111.
8 J. S. Sharp, J. M. Becker and R. L. Hettich, *Anal. Biochem.*, 2003, **313**, 216.
9 C. A. Cohn, M. Borda and M. A. A. Schoonen, *Earth Planet. Sci. Lett.*, 2004, **225**, 271.
10 B. Halliwell and J. M. Gutteridge, *Methods Enzymol.*, 1990, **186**, 1.
11 C. A. Cohn, S. Mueller, E. Wimmer, N. Leifer, S. Greenbaum, D. R. Strongin and M. A. A. Schoonen, *Geochem. Trans.*, 2006, **7**, 3.
12 H. Sies, *Eur. J. Biochem.*, 1993, **215**, 213.
13 S. C. J. Parker, L. Hansen, H. O. Abaan, T. D. Tullius and E. H. Margulies, *Science*, 2009, **324**, 389.
14 J. Kameoka, H. G. Craighead, H. Zhang and J. Henion, *Anal. Chem.*, 2001, **73**, 1935.
15 P. K. Yuen and V. N. Goral, *Lab Chip*, 2010, **10**, 384.
16 H. Y. Park, X. Qiu, E. Rhoades, J. Korlach, L. W. Kwok, W. R. Zipfel, W. W. Webb and L. Pollack, *Anal. Chem.*, 2006, **78**, 4465.
17 B. Breiner, J. C. Schlatterer, S. V. Kovalenko, N. L. Greenbaum and I. V. Alabugin, *Angew. Chem., Int. Ed.*, 2006, **45**, 3666.
18 B. Breiner, J. C. Schlatterer, I. V. Alabugin, S. V. Kovalenko and N. L. Greenbaum, *Proc. Natl. Acad. Sci. U. S. A.*, 2007, **104**, 13016.
19 D. J. Galas and A. Schmitz, *Nucleic Acids Res.*, 1978, **5**, 3157.
20 A. J. Zaug, C. A. Grosshans and T. R. Cech, *Biochemistry*, 1988, **27**, 8924.

21 I. Shcherbakova, S. Mitra, R. H. Beer and M. Brenowitz, *Methods Cell Biol.*, 2008, **84**, 589.
22 H. Summer, R. Gramer and P. Dröge, *Journal of Visualized Experiments*, 2009, **32**, 4.
23 M. Brenowitz, D. Senear, M. Shea and G. Ackers, *Methods Enzymol.*, 1986, **130**, 132.
24 R. Das, A. Laederach, S. M. Pearlman, D. Herschlag and R. B. Altman, *RNA*, 2005, **11**, 344.
25 T. D. Tullius, B. A. Dombroski, M. E. A. Churchill and L. Kam, *Methods Enzymol.*, 1987, **155**, 537.
26 R. Bachu, F. S. Padlan, S. Rouhanifard, M. Brenowitz and J. C. Schlatterer, *Journal of Visualized Experiments*, 2011, DOI: 10.3791/3244, http://www.jove.com/details.php?id=3244.
27 I. Shcherbakova and S. Mitra, *Methods Enzymol.*, 2009, **468**, 31.
28 M. Rhodes, *Introduction to Particle Technology*, JohnWiley & Sons, Ltd, West Sussex, 2nd edn, 2008.
29 A. Donev, I. Cisse, D. Sachs, E. A. Variano, F. H. Stillinger, R. Connelly, S. Torquato and P. M. Chaikin, *Science*, 2004, **303**, 990.
30 A. Jaoshvili, A. Esakia, M. Porrati and P. M. Chaikin, *Phys. Rev. Lett.*, 2010, **104**, 185501.
31 H. J. Cleaves, E. Crapster-Pregont, C. M. Jonsson, C. L. Jonsson, D. A. Sverjensky and R. A. Hazen, *Chemosphere*, 2011, **83**, 1560–1567.
32 J. C. Schlatterer and M. Brenowitz, *Methods*, 2009, **49**, 142.
33 B. Balasubramanian, W. K. Pogozelski and T. D. Tullius, *Proc. Natl. Acad. Sci. U. S. A.*, 1998, **95**, 9738.
34 S. Mitra, I. V. Shcherbakova, R. B. Altman, M. Brenowitz and A. Laederach, *Nucleic Acids Res.*, 2008, **36**, e63.
35 S. M. Vasa, N. Guex, K. A. Wilkinson, K. M. Weeks and M. C. Giddings, *RNA*, 2008, **14**, 1979.
36 J. A. Greenbaum, B. Pang and T. D. Tullius, *Genome Res.*, 2007, **17**, 947.

